ASM Handbook, Volume 6A, *Welding Fundamentals and Processes*
T. Lienert, T. Siewert, S. Babu, and V. Acoff, editors

Numerical Aspects of Modeling Welds*

John Goldak and Mahyar Asadi, Carleton University
Lennart Karlsson, Luleå University of Technology

THE DESIGN OF A STRUCTURE that achieves its highest performance levels with the least chance of failure can be facilitated by the mathematically based prediction modeling of weld behavior in a variety of circumstances. One aspect of a weldment that can be predicted with remarkable accuracy, given certain data, is the transient temperature field. Distortion also can be predicted with considerable accuracy. Although residual stresses and microstructure predictions are less accurate, they are still useful.

At the present time, some aspects of the arc and the weld pool are difficult to predict. Although the prediction of specific defects can be difficult, the conditions that make it likely for specific kinds of defects to form can be predicted. This situation is similar to that of predicting weather conditions that suggest a high risk of tornadoes, but not being able to predict individual tornadoes.

Reality, Models, and Mathematics. Like cartoons, mathematics is not real. Yet, even in cartoons, some relationship to reality is nearly always intended. To understand either cartoons or mathematics, every individual must define his own relationship to reality.

Unlike cartoons, mathematics has two fundamental pillars. A set of axioms, which are sometimes called assumptions, laws, primitives, or other terms, is assumed to be given and to be true. When these assumptions or axioms are combined in ways that obey a strict logic, results remain true, that is, for the purposes of mathematics, rather than for the real world. The meaning of the axioms, as interpreted in the real world, is irrelevant to mathematics. For example, given a sphere of radius r, mathematicians can prove that volume equals $(4\pi r^3)/3$. Whether any particular ball can actually be described or approximated as a sphere of radius r is not a question that mathematics considers. In fact, one cannot prove that the formula for the volume of a sphere is correct by measuring the volume of balls. Rather, the exercise is a matter of judgment and interpretation for those who are interested in the volume of a real ball.

This example is presented in order to show that the confusion and controversy that occur in the modeling of welds and other areas arises from a failure to separate mathematics that are correct from mathematics that represent a useful model for a particular weld. Although this point is often not understood, those who can appreciate it are able to use models more effectively.

Modeling of Welds

The first assumption should be that the weld has been specified, and therefore, all information needed to produce the real weld has been given. This includes the geometry of the welded structure and the weld joint, the composition of the base and weld metal, the distribution of input energy, the preheat temperature, the welding path and speed, the hydrogen content in the arc, the start time and start position of each weld pass, the fixtures, and other factors. It is usually assumed that the transient temperature field is the most critical field, in the sense that if this temperature field is wrong, then the predictions of the model are likely to be wrong. It is also most critical in the sense that different welds usually have different temperature fields. After computing the transient temperature field, the evolution of microstructure in the heat-affected zone and the fusion zone is computed. Then the thermal stress, strain, distortion, and residual stress are computed. The next objective, which is a current research issue, is to predict the mechanical properties of the weldment, including fracture toughness, ductile-brittle transition temperature, and the probability that defects will occur. The ultimate objective is to predict the manufacturing cost and the reliability of both the weld and the welded structure.

Computational weld mechanics described in algorithmic notation comprises the following steps:

- Define the geometry, material properties, heat inputs, boundary conditions such as thermal convection, and mechanical support
- Compute the transient temperature field
- Compute the evolution of microstructure. If latent heats of transformation are to be included, then the transient temperature and evolution of microstructure become an iterative problem.
- Compute the displacement; strain and stress fields, including the effects of temperature and microstructure on material properties; thermal expansion; and phase transformations. Usually, a thermoelastoplastic stress-strain relationship is used. The displacement or distortion can significantly impact the cost of welding.
- Estimate material properties of the weldment, the probability of defects, and the risk of failure due to fatigue, ductile or brittle facture, and corrosion. Although very little research has been published on this step, it is clearly an important objective of computational weld mechanics.

The results of such an analysis are shown in Fig. 1 to 5. It has been assumed that the weld

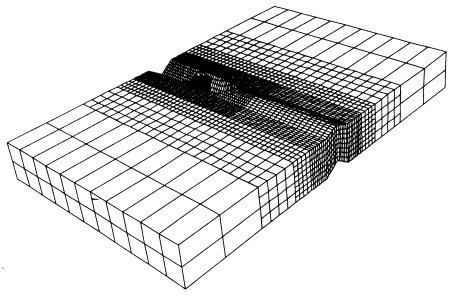

Fig. 1 Finite-element mesh for a weld described in a Eulerian reference frame. Note that filler metal is added. The weld pool, which is not shown, is not needed in this analysis because the temperature is prescribed at the weld-pool boundary. The mesh is finest just in front of the weld pool.

* Revised and updated from J. Goldak, M. Gu, and L. Karlsson, Numerical Aspects of Modeling Welds, *Welding, Brazing, and Soldering,* Vol 6, *ASM Handbook,* ASM International, 1993, p 1131–1140

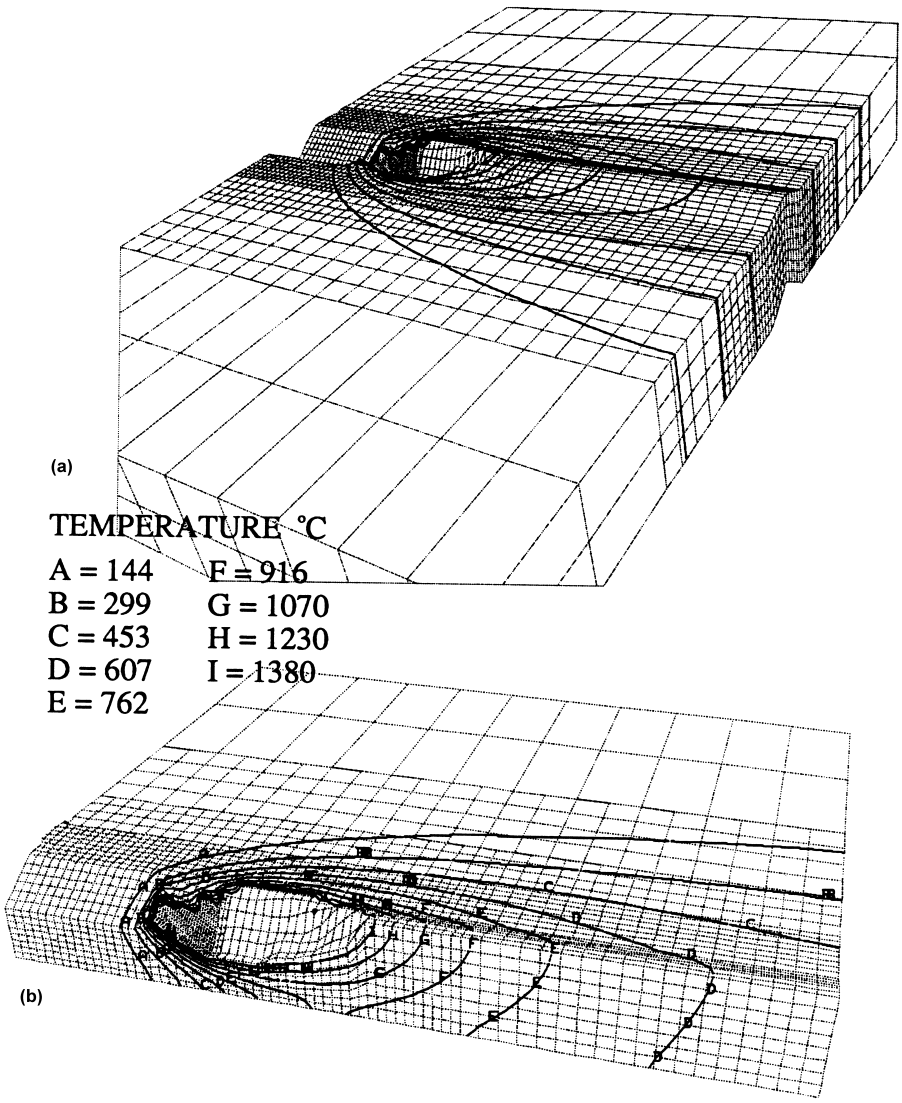

Fig. 2 Temperature contours of a weld in low-carbon steel. (a) For whole mesh. (b) For the region around the weld pool

pool is characterized by known data. The weld pool behavior has not been predicted. In order to predict weld pool behavior, most researchers would assume that the distribution of thermal flux, the current density, and the velocity and pressure in the arc are known data. With these data, they would solve the conservation of mass, momentum, and energy to compute the temperature, velocity, and pressure fields in the weld pool and the position of the weld-pool liquid-solid and liquid-plasma interfaces.

The proceedings of recent conferences in computational weld mechanics are now embodied in the literature (Ref 1–4).

Geometry of Weld Models

Most computational models have analyzed bead-on-plate welds, because of their simple geometry. In addition to bead-on-plate welds, this discussion considers V-groove welds, girth welds, and branch welds on pipes (Fig. 1–9). The geometry specifies the region of space that is to be analyzed. This region is called the domain, Ω, and its boundary is denoted $\partial\Omega$. To analyze the weld, the geometry will usually be represented by a finite-element mesh. Because temperature, stress, and strain change rapidly near the weld, it is useful to use a fine mesh near the weld for resolution and accuracy. However, a coarse mesh is preferred at a site far from the weld, in order to reduce computational costs without unduly sacrificing accuracy or resolution. For this reason, it is desirable to have the ability to grade the mesh or to adaptively refine and coarsen a finite-element mesh for analyzing welds (Ref 5).

Energy Equation and Heat Transfer

The conservation of energy is the fundamental principle that underlies all thermal analysis, including that of welds. In the simplest terms, it states that while energy can be added or extracted, no energy can be created or destroyed in the domain being analyzed. The essential material behavior for heat conduction is that a flux of energy, q (J/m^2 · s), flows from hot regions to cold regions under the influence of a temperature gradient, ∇T, and the thermal conductivity of the material, κ:

$$q = -\kappa \nabla T \quad \text{(Eq 1)}$$

The energy required to change the temperature of a material is defined by another material property, the specific heat, C_p, or enthalpy, H, of a material. The enthalpy is defined with respect to a reference temperature, T_{ref}, as:

$$H(T) = \int_{T_{ref}}^{T} C_p \, dT \quad \text{(Eq 2)}$$

In terms of the enthalpy, thermal flux, and a distributed heat-source term, S (J/m^3 · s), the energy equation in differential form is:

$$H - \nabla \cdot q - S = 0 \quad \text{(Eq 3)}$$

or, in terms of temperature, it is:

$$\rho C_p T - \nabla \cdot (-\kappa \nabla T) - S = 0 \quad \text{(Eq 4)}$$

This is a parabolic partial differential equation. The essential parts of any such equation are the boundary conditions, the initial conditions, and the parameters such as specific heat, C_p, thermal conductivity, κ, and heat source per unit volume, S. The boundary conditions can be either essential (prescribed temperature) or natural (prescribed thermal fluxes) for all time. The part of the boundary on which essential boundary conditions are prescribed is called $\partial\Omega_D$, whereas the part of the boundary on which natural boundary conditions are prescribed is called $\partial\Omega_N$. These two parts must make up the entire boundary, and they must not overlap at any point, that is, at no point can both be essential and natural. In mathematical terms, this is expressed as $\partial\Omega = \partial\Omega_D \cup \partial\Omega_N$ and $\partial\Omega_D \cap \partial\Omega_N = \emptyset$. The essential boundary condition is:

$$T(x,t) = F_D(x,t), \; x \in \partial\Omega_D, t > 0 \quad \text{(Eq 5)}$$

and the natural boundary condition is:

$$q(x,t) = F_N(x,t), \; x \in \partial\Omega_N, t > 0 \quad \text{(Eq 6)}$$

The initial conditions describe the distribution of temperature or enthalpy at all points in the interior of the domain, Ω, at time zero:

$$T(x,t) = F_{init}(x), \; x \in \Omega, t = 0 \quad \text{(Eq 7)}$$

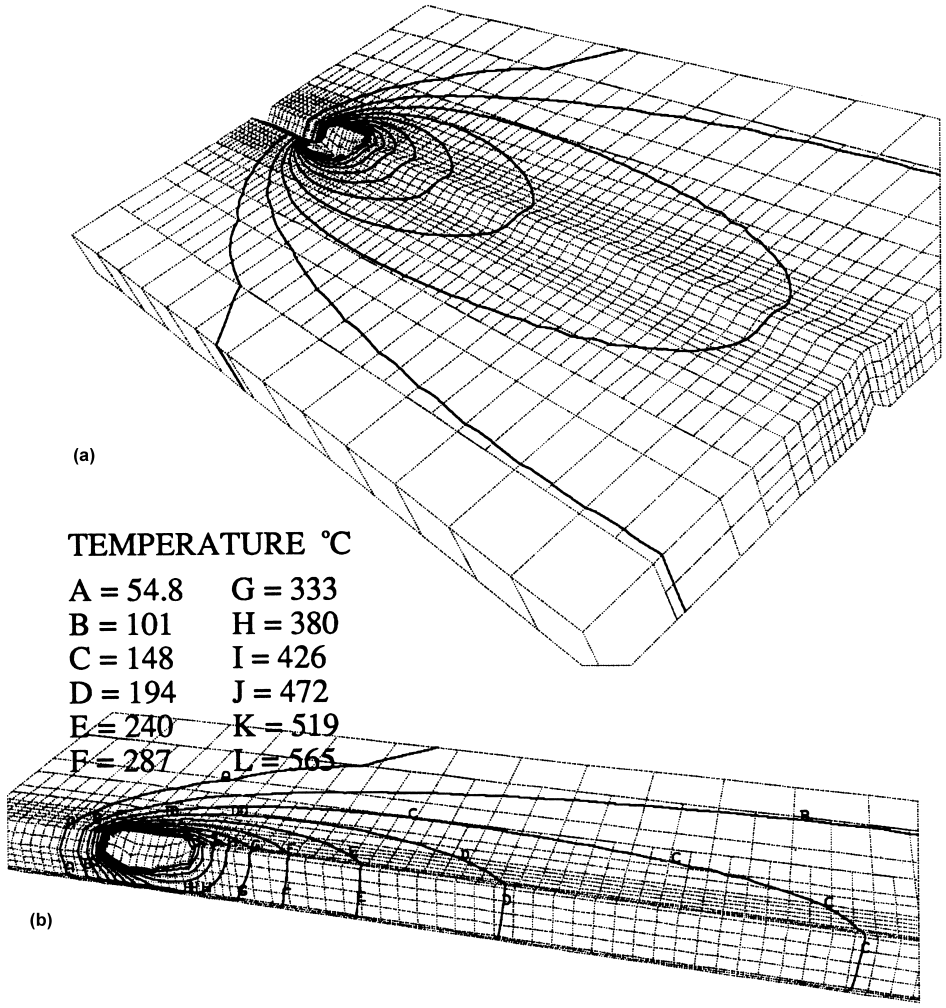

Fig. 3 Temperature contours of a weld in aluminum alloy. (a) For whole mesh. (b) For the region around the weld pool. Because the thermal diffusivity of aluminum is higher than steel, the mesh can be coarser, particularly in front of the weld pool.

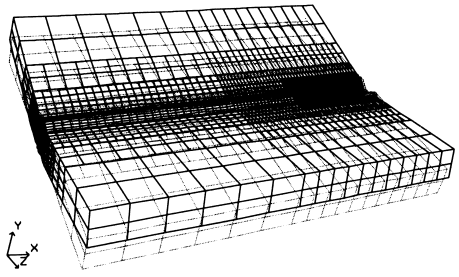

Fig. 4 Distortion (magnified by a factor of 2) of a steel plate

If the latent heat of phase transformations is to be considered, then the initial distribution of the density of each phase, ρ_i, is also needed:

$$\rho_i(x,0) = \rho_{i_{init}}(x),\ x \in \Omega, t = 0 \qquad \text{(Eq 8)}$$

The known functions, that is, data, are F_D, F_N, F_{init}, and ρ_{init}.

To include the effect of phase transformations, such as liquid to solid and the decomposition of austenite in low-alloy steels, it would be necessary to have equations describing the evolution of each phase. However, this has not been included in this energy equation. The latent heat of solid-state transformations, such as austenite to ferrite in steel, has a detectable effect on the temperature field, but it is not large. To date, this effect has not played an important role in the thermal analysis of welds.

Solving the Energy Equation. The energy equation defined previously can now be solved for a specific welding situation. Finite-element methods (FEMs) have been the method of choice for stress analysis. Finite-difference methods (FDMs) have been the method of choice for fluid flow. Whether the FDM or FEM method is best is an old argument. In rough terms, FEM has been used more frequently for complex geometries and for stress analysis, whereas FDM has been used more frequently for fluid-flow analysis. However, FDM can be used for complex geometries that use body-fitted coordinates. Some have argued that FDMs are computationally more efficient than FEMs. The computational efficiency depends on the implementation. There is no fundamental reason why one method should have a computational advantage. The FEM is used here because of its familiarity and because it is better established for stress analysis.

The FDM directly discretizes the partial differential equation by approximating derivatives with finite-difference expressions. The FEM transforms the partial differential equation to an integral form and then approximates the integrals. A Green's identity is usually used to reduce the degree of the highest derivative from order two to order one. In addition, it introduces the natural boundary conditions in a natural and elegant manner. The resulting integrals are approximated by a finite set of basis functions, usually piecewise polynomials. The piecewise polynomials can be interpreted as being defined by choosing a mesh of elements and nodes. Within each element, a polynomial is chosen for each node. Usually, it has a value of 1 for its node and a value of 0 at all other nodes in the element.

These basis functions can be used to interpolate the temperature field by using the value of the temperature at each node. For example, if the (x,y) nodal coordinates of a triangle are (1,0), (0,1), (0,0), and the basis functions for a triangle are chosen to be $\varphi_1(x,y) = x$; $\varphi_2(x,y) = y$; and $\varphi_3(x,y) = 1 - x - y$, then the temperature at any point (x,y) in the element can be expressed as:

$$T(x,y) = \varphi_1(x,y)T_1 + \varphi_2(x,y)T_2 + \varphi_3(x,y)T_3 = \sum_{i=1}^{3} \varphi_i(x,y)T_i \qquad \text{(Eq 9)}$$

where T_i is the temperature at node i. Note that if distorted triangles are used, then understanding the mathematics becomes more complex, because the polynomial basis functions are distorted into rational functions. If the distortion is excessive, then the basis functions can become singular. However, distorted elements do not make FEM programs more difficult to use, as long as the distortion is not excessive.

To solve the energy equation defined previously, FEM can be interpreted as minimizing a potential, solving a variational problem, projecting an exact solution from an infinite dimensional space onto a finite dimensional space, or finding the best approximation to the exact solution in the finite dimensional space in some least-squares sense. All of these interpretations lead to the same set of ordinary differential equations, which can then be converted to the same set of algebraic equations in order to solve:

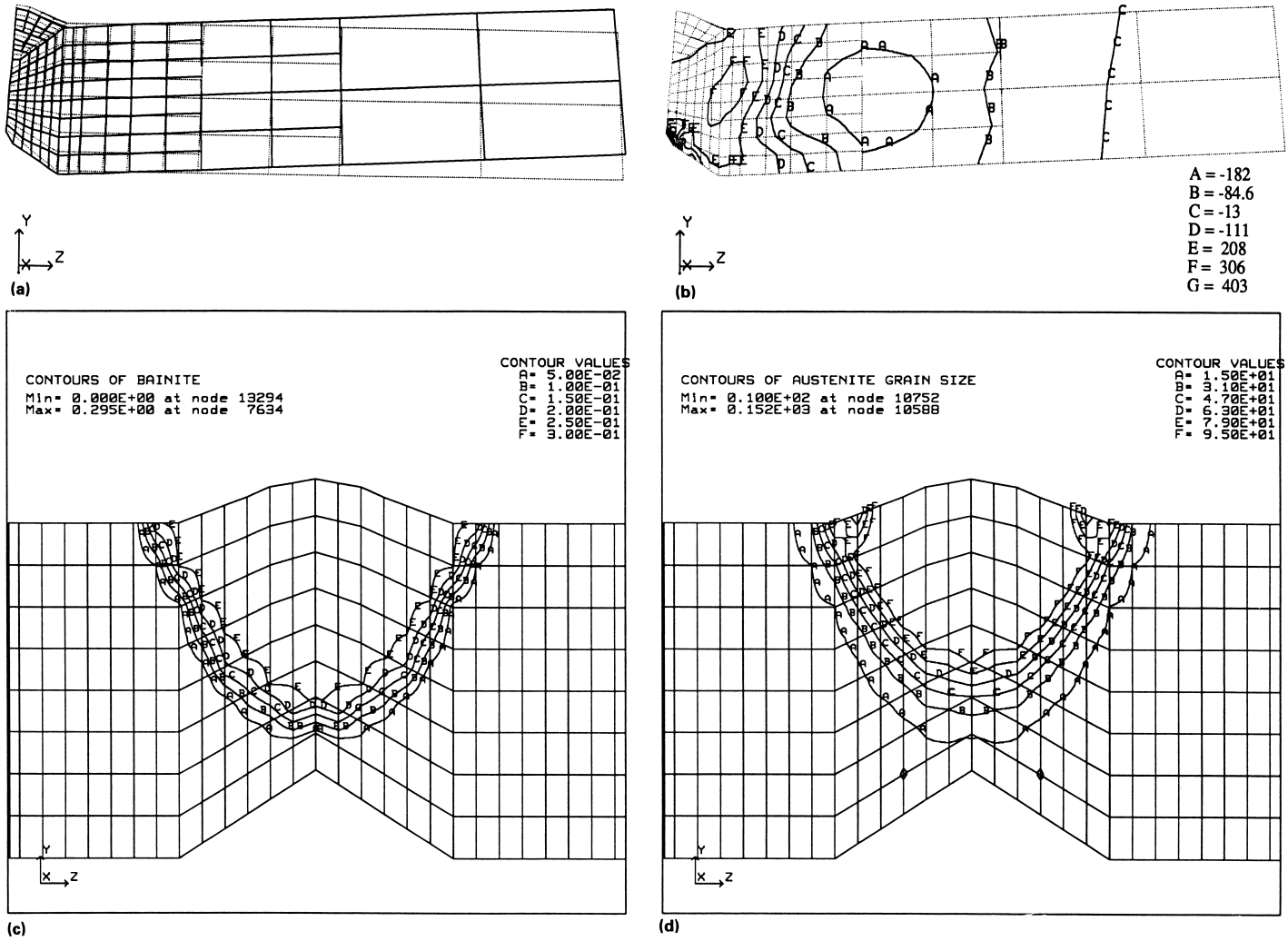

Fig. 5 (a) Distortion of weld shown in a cross section. Note the rigid body motion of the region far away from the weld nugget. (b) Contours of the longitudinal residual-stress component, σ_{xx}. Note that the maximum stress is not located at the surface. (c) Contours of fraction of bainite at end of weld; maximum fraction of bainite is just under 0.3. (d) Contours of prior-austenite grain size at the end of weld

$$\left(\bar{C}_p \frac{G}{\delta} + \theta K\right)\Delta T = S^1 - KT^1$$
$$-\tilde{N}(U)H^1 \rightarrow K_{eff}\Delta T = b_{eff} \qquad \text{(Eq 10)}$$

where $\bar{C}_p$ is the specific heat per unit volume, G is the gram matrix, δ is the length of the time step, θ is a parameter that determines the time-integration method, $\Delta T = T^3 - T^1$ is the increment in the temperature in this time step, S^1 is the nodal load vector that is due to external thermal loads, $\tilde{N}(U)H^1$ is the nodal load vector that is due to advection evaluated at the beginning of the time step, K_{eff} is the effective stiffness matrix, and b_{eff} is the effective load vector.

For a detailed presentation of FEM theory, refer to any textbook on the subject, such as Ref 6 to 8. Space constraints here do not allow a more detailed explanation. Because commercially competitive FEM programs typically require hundreds of man-years to write, as well as special expertise, it is assumed that most readers will choose not to write an FEM program, but will use an FEM program written by others. When choosing an FEM program, four main issues should be considered: functionality, computational efficiency, ease of use, and ease of learning. Because most of the costs of analysis are in preparing data and training, the latter two issues are nearly as important as functionality.

Convection, Radiation Boundary Conditions, and Contact Conductance. Given a body at temperature T immersed in a fluid at temperature T_{amb}, convection assumes that a thermal boundary layer exists with conductance, h (J/m^2 · s · °C), such that the temperature difference across the boundary layer causes a flux, q (J/m^2 · s), given by:

$$q_{con} - h(T - T_{amb}) \qquad \text{(Eq 11)}$$

If the fluid is flowing with velocity, v, and pressure, p, over a plate with a Prandtl number, Pr, and a Reynolds number, Re, then the convection coefficient can be estimated to be:

$$h = 0.332\,\frac{\kappa}{\lambda}\,\mathrm{Re}^{1/3}\,\mathrm{Pr}^{1/3} \qquad \text{(Eq 12)}$$

Given a body at temperature T radiating to a body at temperature T_{amb}, radiation assumes an emissivity and Stefan-Boltzmann constant, σ (J/m^2 · s · K^4), such that the temperature difference causes a flux, q (J/m^2 · s), given by:

$$q_{rad} = \epsilon\sigma\left(T^4 - T_{amb}^4\right) \qquad \text{(Eq 13)}$$

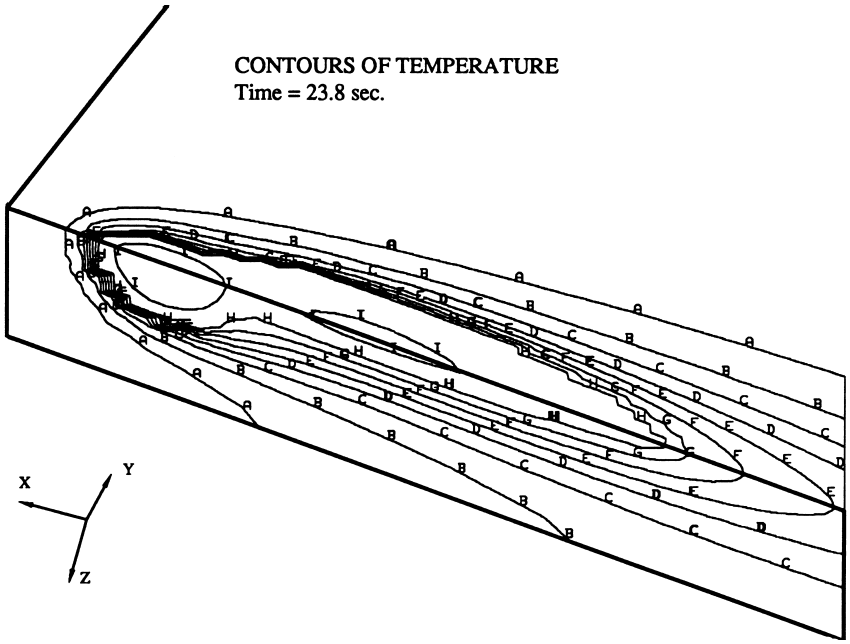

Fig. 6 Temperature isotherms near the weld pool in Barlow's weld. Note that contour "I" has two pools: one under the arc and one in the region behind the arc. This heat source was modeled as a prescribed-temperature region.

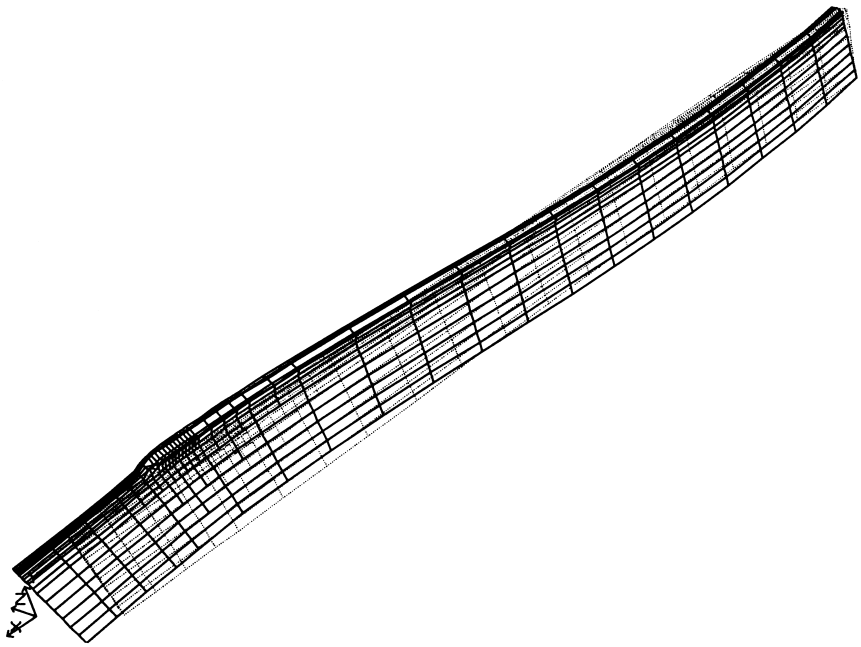

Fig. 7 Distortion of a bar being welded. Note the change of curvature. Near the weld pool, the center of curvature is below the bar. Far behind the weld pool, the center of curvature is above the bar.

This is usually linearized as:

$$q_{\text{rad}} = \epsilon\sigma\left(T^2 + T_{\text{amb}}^2\right)(T + T_{\text{amb}})(T - T_{\text{amb}}) \equiv h_{\text{rad}}(T - T_{\text{amb}}) \quad \text{(Eq 14)}$$

Then, the effects of radiation and convection can be combined into a single effect if the ambient temperatures are equal. Of course, the ambient temperature for convection and radiation need not be equal.

In an FEM program, this boundary condition is applied by specifying the values of the convection coefficient and the ambient temperature at the nodes on this part of the boundary. The program computes a contribution to the nodal thermal load and the stiffness matrix.

Modeling the Heat Source in a Weld. Rosenthal (Ref 9) and Rykalin (Ref 10) modeled the heating effect of the arc traveling on a thick plate as a point source; that is, they assumed that all the energy is input into a point. In an FEM model, this could be approximated by specifying a thermal load at a node shared by very small elements.

It is worth exploring the difference between the FEM approximation and the Rosenthal solution for the point source. The most notable difference is that the temperature at the point source is infinite in the Rosenthal solution, whereas it is finite in the FEM approximation. The explanation is that in the Rosenthal solution, a finite amount of energy is being put into zero volume at the point. This causes an infinite temperature. In the FEM approximation, a finite amount of energy is being put into the elements containing the node, which is the point source. Because these elements have a finite volume, the temperature is finite.

If the temperature is plotted near the point source, the Rosenthal solution varies exponentially with position. The FEM solution has a polynomial dependence on position that comes from the polynomial basis functions. If the finite-element mesh size goes to zero, then the FEM approximation to the Rosenthal solution becomes more accurate.

Rosenthal and Rykalin chose a point source, not because they believed the arc was of zero size, but because it enabled them to solve the energy equation. Their solution was a useful approximation at points that were sufficiently accurate far from the arc. With the FEM, there is no advantage in choosing a point source. It is preferable to use a more-accurate approximation to the energy distribution in the arc.

Pavelic et al. (Ref 11) used a truncated Gaussian distribution of a prescribed flux in a circular disk moving with the arc over the weld joint. This can be accurate as long as the arc does not suppress the weld-pool surface too much and convection effects in the weld pool are not too large. If the arc-pool surface depression is large and/or if the velocity in the weld pool is large, then it can be more accurate to model the heat input, not as a distributed flux but as a distributed power density heat source that defines the heat input per unit volume per unit time at each point in the weld-pool region.

Goldak et al. (Ref 12) proposed a truncated Gaussian distributed heat source in a double-ellipsoid region. More-complex weld-pool shapes can be approximated by superimposing distributed heat sources.

Various phenomena can be introduced into these heat-source models, such as radiation, evaporation, and latent heat of fusion. However, it is useful to perform the following thought experiment to clarify their role. Assume that the exact temperature field is known as a function of time. Now, prescribe

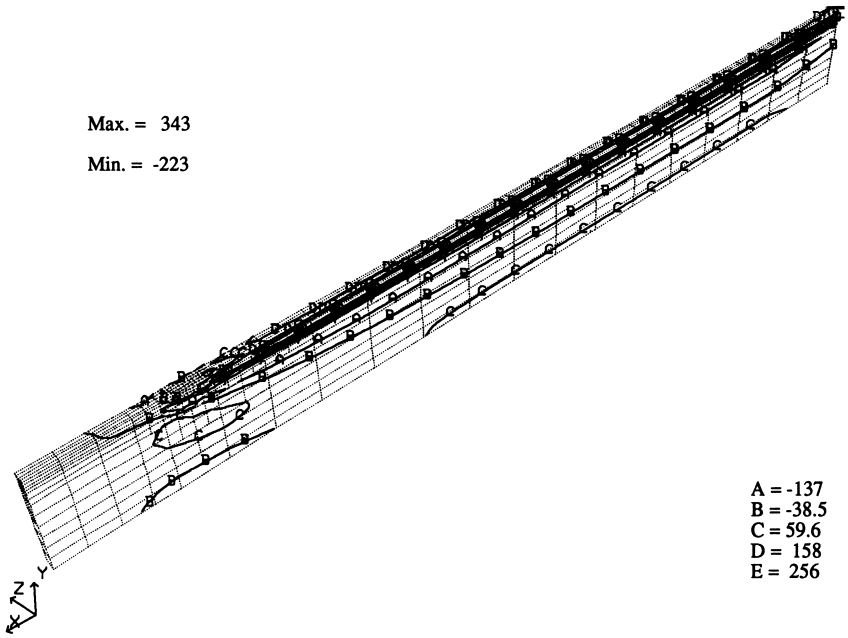

Fig. 8 Contours of the longitudinal stress for the weld shown in Fig. 7

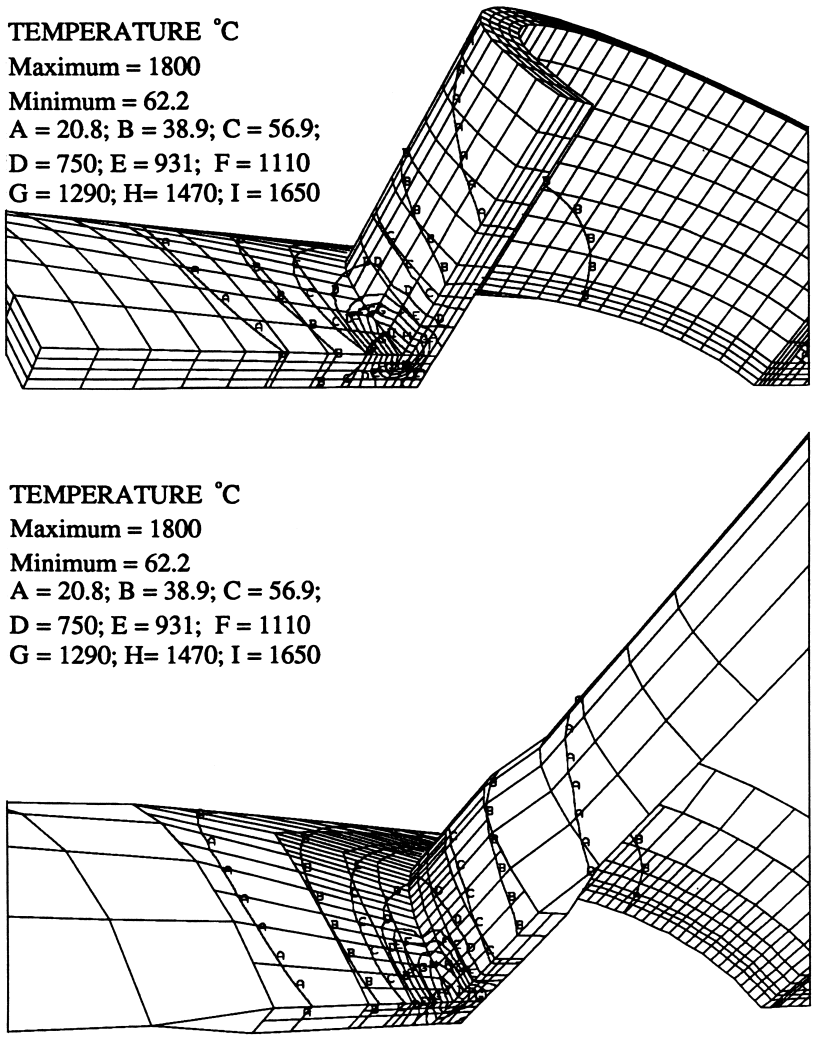

Fig. 9 Cutaway views of a branch pipe or T-joint weld. Top figure uses only eight node bricks. Note that the temperature gradient through the thickness of the pipe is negligible, except near the weld pool. The mesh in the bottom figure uses thermal shell elements and is both more accurate and more efficient.

that temperature field in the FEM equation. The reaction at each node is the nodal thermal load, which includes the net effect of all such phenomena. This can be for any shape of weld pool. Therefore, these phenomena can be included implicitly in the distributed heat source model, if desired, or they can be treated separately. If they are treated separately, then the definition and value of the distributed heat source should be changed accordingly.

Prescribed-Temperature Heat Source. If an estimate of the temperature in the weld pool is available, then it is often more convenient to model the heat source by prescribing the temperature in the weld-pool region (Ref 13). For example, the temperature on the surface of the weld pool and a cross section of the weld nugget could be measured. The liquid-solid interface could be assumed to be at or slightly below the solidus temperature. Then, nodes in the weld-pool region could have their temperatures prescribed. The reactions at these nodes would be the prescribed nodal thermal load that produces the same temperature distribution. Thus, the prescribed-temperature heat-source model and the prescribed distributed thermal load heat source are equivalent in the sense that either can be used to produce the same temperature solution. The experience of the authors has shown that estimating the prescribed-temperature distribution is much easier than estimating the distributed heat source, particularly for complex weld-pool shapes. For example, the authors were not able to estimate a distributed power density source that could model the weld shown in Fig. 6, whereas modeling this weld with a prescribed-temperature source was not difficult.

Material versus Spatial Reference Frames. Although Rosenthal used a spatial reference frame, most FEM analyses of welds have used a material reference frame. A spatial frame is fixed in space, and any space can be chosen. Rosenthal chose a space that was tied to the arc. It may be easiest to visualize this as an arc that is fixed in space, where the plate being welded moves under the arc through the spatial mesh. It is equally valid to imagine the plate fixed in one space and the arc fixed in a second space. In this case, Rosenthal used the second space.

A material reference frame defines the configuration of the body either at some point in time (usually, time zero) or at the beginning of each time step. The displacement field defines the mapping from the reference configuration to the configuration of the body at any other time. Imagine that each node in a finite-element mesh is associated with a material point. The node and its associated material point move through space as a function of time. This defines a material reference frame.

Most FEM analyses of welds have used a material reference frame, also called a Lagrangian reference frame, in which the heat source moves as a function of time. However, because the FEM is discretized in time, the usual FEM analysis is equivalent to a series of spot welds. If the time steps are sufficiently small so that

the distance the heat source moves in one time step is sufficiently small, such as half its diameter, then the effect of this discretization need not be excessive. If the time step is so large that the heat source moves more than, say, three times its diameter, for example, then the difference between the computed and measured temperature field will be large.

The use of a spatial frame, which is often called a Eulerian frame, avoids this problem. However, it introduces an advective term into the FEM equation. This term is nonlinear, and the usual formulation leads to an asymmetric set of equations to solve. Recently, Gu (Ref 14) implemented the Eulerian formulation and demonstrated its advantages (Fig. 1–5). The spatial frame enables longer time steps to be taken as the weld approaches steady state.

Transient versus Steady State. In a spatial frame that is tied to the heat source, the temperature near the arc of a long weld parallel to the prismatic axis of a prismatic body soon reaches a steady state. Indeed, the Rosenthal solution is an example of such a steady state. The weld pool typically reaches steady state in one to three weld-pool lengths. A rough guide is that any isotherm will approach the steady state in one to three isotherm lengths. Thus, lower temperatures require longer times and longer lengths to reach steady state. In analyzing long prismatic welds, computational efficiency can be gained by analyzing the steady state. Leblond et al. (Ref 15) and Gu (Ref 14) provide details, and the results of a steady-state analysis are shown in Fig. 1 to 5.

Modeling the Addition of Filler Metal. Bead-on-plate welds can have the simplest geometry and meshes, and they can exploit symmetry to reduce computing costs. When joint details are included, the mesh is somewhat more difficult to create. If welds are not on the symmetry plane, then symmetry cannot be exploited and the computational cost increases. These difficulties are minor, when compared with the difficulties of modeling the addition of filler metal. The first models used a material reference frame, created a mesh, and then turned on or activated those elements to which filler metal was added as they filled (Ref 14, 16). When it is applicable, a spatial frame offers a more-elegant approach, because the weld pool can be fixed or varied slowly, as desired (Ref 14) (Fig. 6). Figures 2 and 3 show the transient temperature field in a groove weld with added filler metal.

Microstructure Evolution

Microstructure strongly affects the material behavior and hence constitutive parameters, such as thermal conductivity, specific heat, and Young's modulus. Volume changes associated with phase changes, such as austenite to ferrite, can cause large strains. For these reasons, microstructure can have a dominant effect in the stress analysis of a weld.

This discussion is limited to welds in low-alloy steels. The phase, or equilibrium, diagram identifies the phases that are present, their composition, and the fraction of each phase present in a steel as a function of alloy composition, temperature, and pressure. Because as many as 10 alloying elements can be significant in low-alloy steel, the phase diagram could be in a space of 11 dimensions. To make this more tractable, this discussion uses pseudobinary iron-carbon diagrams. As functions of composition, the Ae_3 (austenite to austenite-ferrite line) and Ae_1 (eutectoid) temperatures are of particular interest when analyzing the decomposition of austenite.

At each temperature, the system tends to equilibrium. Phases that are unstable tend to transform to stable phases. Although the direction is largely controlled by thermodynamics, the rate is largely governed by kinetics. Following Kirkaldy (Ref 17), it is assumed that the decomposition of austenite into ferrite, pearlite, and bainite can be described by ordinary differential equations of the form:

$$\frac{df}{dt} = B(G,T)f^m(1-f)^p \qquad \text{(Eq 15)}$$

where $(1-f)$ is the fraction of austenite; f is the fraction of the transformation product, for example, ferrite; the function $B(G,T)$ reflects the influence of grain size, undercooling, the alloy and temperature dependence of the solute diffusivity, and the phase fractions that are present; and m and p are parameters of the alloy system. This is essentially the model that was developed by Henwood et al. (Fig. 10). It was used to compute the microstructures in the heat-affected zone (HAZ) of the problems analyzed in Ref 19. Vandermeer (Ref 20) has proposed a modification to include the effect of carbon accumulation in the austenite during the transformation.

Austenite grain growth in the HAZ is computed from the ordinary differential equation:

$$\frac{dG}{dt} = \frac{1}{2G}ke^{-Q/RT} \qquad \text{(Eq 16)}$$

where G is the austenite grain size, k is a parameter, Q is the activation energy, R is the

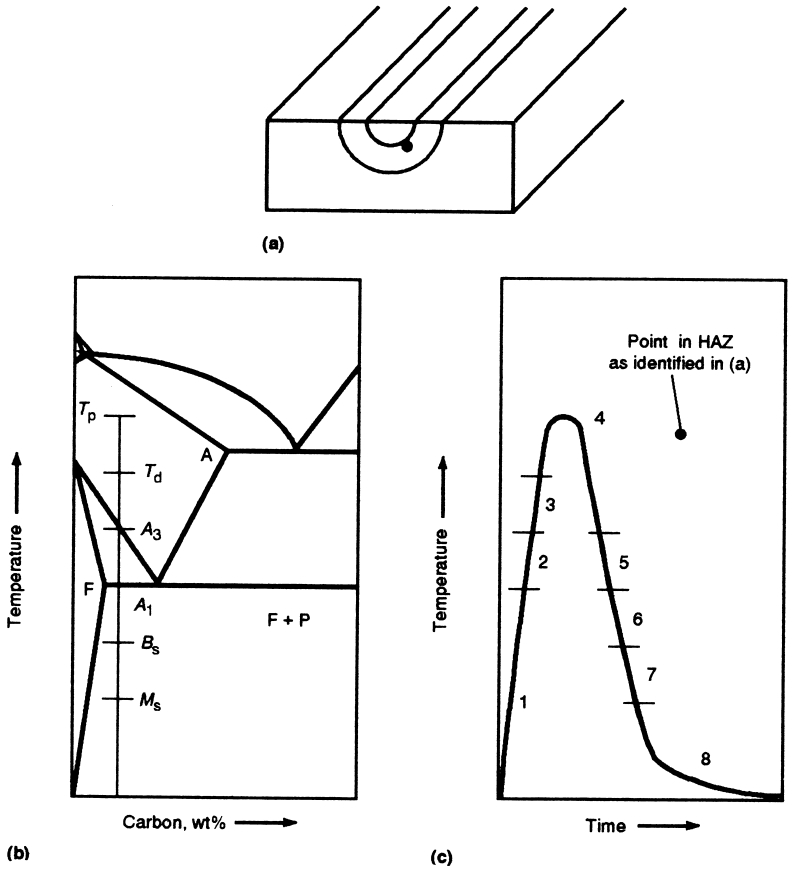

Fig. 10 (a) Schematic cross section of a bead-on-plate weld, identifying a point in the heat-affected zone (HAZ). (b) Iron-carbon phase diagram, identifying the cooling path and critical temperatures. (c) Thermal cycle, identifying the regions that must be considered when implementing the microstructure algorithm. Source: Ref 18

universal gas constant, and T is the absolute temperature. The grain size of austenite has a dominant effect on the hardenability of steel and hence the decomposition of austenite. The authors suspect that errors in the predicted austenite grain size are a significant cause of errors in the evolution of microstructure in the HAZ. In particular, this grain size is the average grain size. The equation was developed for grain growth in annealing essentially homogeneous regions. In a heterogeneous HAZ with steep temperature gradients across single grains, it is not clear that this equation is appropriate (Ref 21).

The aforementioned microstructure models, with the exception of that proposed by Vandermeer, do not consider the composition of each phase or the composition changes that are due to solute diffusion between phases. They only consider the composition of the system. Phase fractions are density functions that specify the mass fraction of a phase per unit volume. Grain size is also a density function. Thus, there is no representation of the microstructure and no capability to draw the microstructure being analyzed.

Thermal Stress Analysis of Welds

Stress analysis deals with the equilibrium of forces, the kinematics of deformation, and the relationship between deformation and force. The existence of a stress tensor field, a strain tensor field, a displacement vector field, and a constitutive relationship between stress and strain are assumed. The conservation of momentum is the fundamental conservation law.

From another viewpoint, the equilibrium of forces is expressed by the conservation of momentum and the definition of the stress tensor, σ, the traction vector, τ, and the body force, b, in the differential equation:

$$\nabla \cdot \sigma + b = m\ddot{x} \qquad \text{(Eq 17)}$$

In welding, it is typical to assume that the inertial forces are negligible, that is, $m\ddot{x} \approx 0$. This implies that the rate of change of loads is small, relative to the time required for a stress wave to propagate across the domain and for a stress wave to decay.

The solvability equations require the integrals of the external forces, that is, the traction vector, τ, and the body force, b, to be in equilibrium with themselves:

$$\int_{\Omega} b\, d\Omega + \int_{\partial\Omega} \tau\, d\Omega = 0 \qquad \text{(Eq 18)}$$

Whether or not the deformed body is rigid, the external forces must be in equilibrium.

The kinematics or deformation is described by the displacement and strain fields. For a total displacement field, $[u,v,w]^{\mathrm{T}} = [u(x,y,z,t),\ v(x,y,z,t),\ w(x,y,z,t)]^{\mathrm{T}}$, at the point (x,y,z,t), the Green's strain is defined as:

$$\epsilon = \frac{\nabla u + \nabla u^{T} + \nabla u^{T} \nabla u}{2} \qquad \text{(Eq 19)}$$

where ∇u is the deformation gradient:

$$\nabla u = \begin{bmatrix} \frac{\partial u}{\partial x} \frac{\partial v}{\partial x} \frac{\partial u}{\partial x} \\ \frac{\partial u}{\partial y} \frac{\partial v}{\partial y} \frac{\partial w}{\partial y} \\ \frac{\partial u}{\partial z} \frac{\partial v}{\partial z} \frac{\partial w}{\partial z} \end{bmatrix} \qquad \text{(Eq 20)}$$

The Green's strain is a symmetric tensor. It measures the change in distance between points in the neighborhood of a point caused by the deformation.

The material properties are described by the constitutive, or stress-strain, relationship, $\sigma = D\varepsilon$, where D is the fourth-order tensor that maps the elastic strain tensor to the stress tensor. Thermodynamic arguments require D to be symmetric positive definite. For isotropic elastic materials, D is defined by two constants, such as Young's modulus and Poisson's ratio.

Most FEM analyses of welds have used an additive decomposition of the total strain rate into elastic, thermal, plastic, and transformation plasticity strain rates:

$$\dot{\epsilon}^{\mathrm{Tot}} = \dot{\epsilon}^{\mathrm{Elas}} + \dot{\epsilon}^{\mathrm{Therm}} + \dot{\epsilon}^{\mathrm{Plas}} + \dot{\epsilon}^{\mathrm{TransPlas}} \qquad \text{(Eq 21)}$$

Plasticity theory and numerical algorithms based on the multiplicative decomposition of the deformation gradient $\mathbf{F} = \mathbf{F}^{\mathrm{e}}\mathbf{F}^{\mathrm{p}}$ were developed in the period 1985 to 1994 (Ref 22). This theory is better suited to finite strain analyses. Although the creep strain rate could be included, the authors are not aware of published studies of creep in the modeling of welds, to date.

Equation 18 is an elliptic partial differential equation. Boundary conditions are an essential part of any such equation, and they can be either essential (prescribed displacement) or natural (prescribed traction). They must be prescribed for all time. The part of the boundary on which essential boundary conditions are prescribed is called $\partial\Omega_{\mathrm{D}}$, whereas the part of the boundary on which natural boundary conditions are prescribed is called $\partial\Omega_{\mathrm{N}}$. These two parts must make up the entire boundary, and they must not overlap at any point. In mathematical terms, this is expressed as $\partial\Omega = \partial\Omega_{\mathrm{D}} \cup \partial\Omega_{\mathrm{N}}$ and $\partial\Omega_{\mathrm{D}} \cap \partial\Omega_{\mathrm{N}} = 0$. The essential boundary condition is:

$$u(x,t) = F_{\mathrm{D}}(x,t),\ x \in \partial\Omega_{\mathrm{D}}, t > 0 \qquad \text{(Eq 22)}$$

The natural boundary condition is:

$$\tau(x,t) = F_{\mathrm{N}}(x,t),\ x \in \partial\Omega_{\mathrm{N}}, t > 0 \qquad \text{(Eq 23)}$$

Although an elliptic boundary value problem does not have initial conditions, initial data describing the distribution of the displacement, strain, or stress can be specified at all points in the interior of the domain, Ω, at time zero:

$$\begin{aligned} \sigma(x,t) &= F_{\sigma\mathrm{init}}(x),\ x \in \Omega, t = 0 \\ \epsilon(x,t) &= F_{\epsilon\mathrm{init}}(x),\ x \in \Omega, t = 0 \\ u(x,t) &= F_{u\mathrm{init}}(x),\ x \in \Omega, t = 0 \end{aligned} \qquad \text{(Eq 24)}$$

If microstructure evolution is considered, then only the macroscopic (average) stress, strain, and displacement fields will be considered. In other words, the variations in the fields, below some length scale, are averaged or ignored. This is inherent in a finite-element mesh, because an FEM analysis cannot detect spatial frequencies higher than those captured by the polynomials in the mesh.

Given the transient temperature-rate field in a weld, the thermal volumetric strain rate is:

$$\begin{aligned} \dot{\epsilon}^{\mathrm{Therm}} &= \bar{\alpha}\dot{T} \\ \delta t\, \dot{\epsilon}^{\mathrm{Therm}} &\approx \Delta\epsilon^{\mathrm{Therm}} = \alpha\Delta T \\ \bar{\alpha} &= \alpha + \frac{\mathrm{d}\alpha}{\mathrm{d}T}(T - T_{\mathrm{ref}}) \end{aligned} \qquad \text{(Eq 25)}$$

The coefficient of thermal expansion, α, is a property of the material.

If the stress, body force, traction, strain, and displacement fields are sufficiently smooth, then this is a well-posed problem and the mathematics is well understood. The aforementioned continuum mechanics problem can be solved by an FEM approximation. In particular, the total strain rate is approximated by:

$$\dot{\epsilon}^{\mathrm{Tot}} = B\dot{u} \qquad \text{(Eq 26)}$$

where $\dot{u}$ is the nodal displacement rate or velocity, and B is the discrete symmetric gradient operator.

Examples of stress analysis of welds are shown in Fig. 7 and 8. For a general reference on continuum mechanics and stress analysis, refer to Ref 23 and 24.

Transformation Plasticity. Although the transformation of austenite to ferrite, pearlite, bainite, and martensite causes only a small effect on the temperature field, it can have a major effect on the stress field. This arises through the phenomenon of transformation plasticity (Ref 25, 26). The rate of transformation of austenite, $\dot{Z}$; the deviatoric stress, τ_{ij}, and constant, K, that includes the volume change associated with the phase change; and the yield strength all determine a contribution to the strain rate and strain increment, given by:

$$\dot{\epsilon}_{ij}^{\mathrm{TransPlas}} = K\tau_{ij}\dot{Z} \quad \Delta\epsilon_{ij}^{\mathrm{TransPlas}} = \int_{t1}^{t2} K\tau_{ij}\dot{Z}\mathrm{d}\xi \qquad \text{(Eq 27)}$$

This effect is greatest in high-strength steels such as HY-80 because the decomposition of austenite occurs at lower temperatures, where the volume change associated with the phase change is largest (Fig. 11). In addition, plastic deformation that occurs after the phase transformation is complete tends to hide or blur the effects of transformation plasticity. When the transformation occurs closer to room temperature, the effects of transformation are blurred

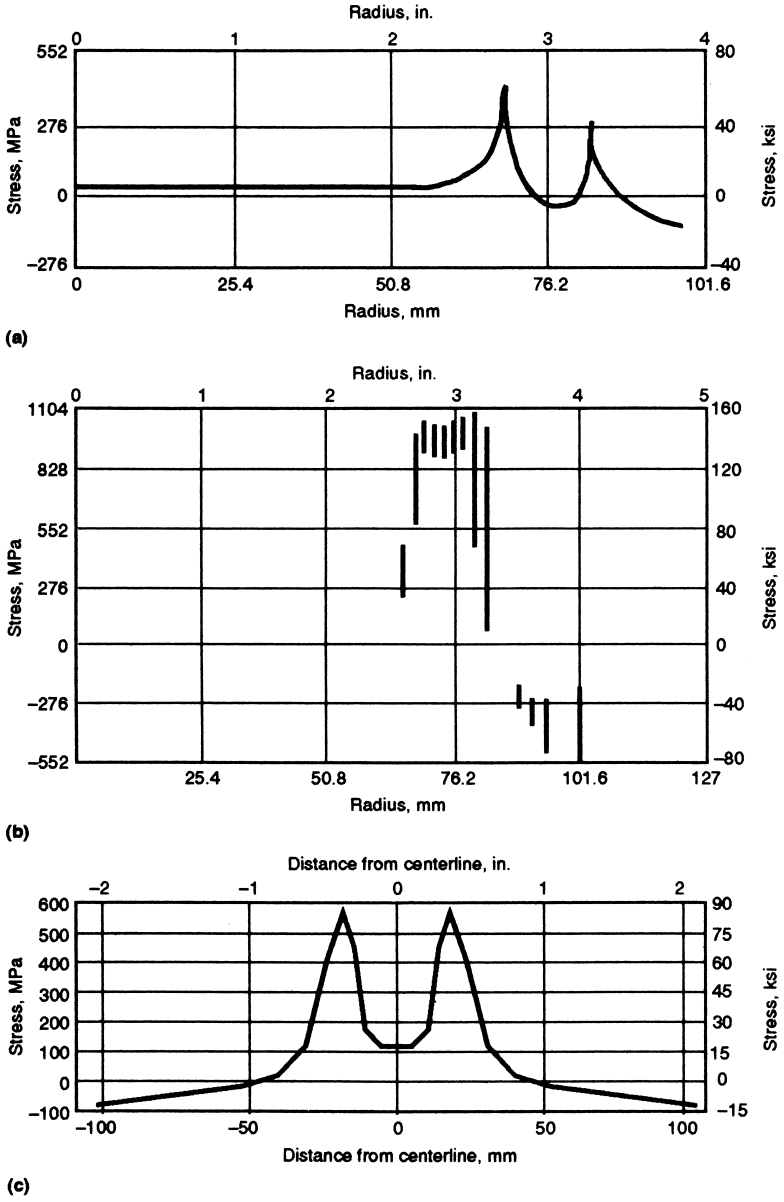

Fig. 11 (a) Experimental data published by Corrigan (Ref 27) for the residual stress in an HY-130/150 weld. (b) Predicted values of residual stress, published by Hibbitt and Marcal (Ref 28), who ignored the austenite-to-martensite transformation in their finite-element method (FEM) analysis of the residual stress. (c) Predicted values of longitudinal residual stress, as predicted by FEM analysis of Oddy (Ref 26), who has taken into account the effects of the phase transformation and transformation plasticity. Clearly, the effects of the phase transformation dominate the stress analysis in this case.

the least. In lower-strength steels and higher weld heat inputs, the transformation of austenite tends to occur nearer the eutectoid temperature, and the effect on the final residual-stress state is less pronounced.

Because the transformation plastic strain rate strongly affects the deviatoric stress, and because the deviatoric stress strongly affects the transformation plastic strain rate, the integration of Eq 27 requires some care in order to avoid instability. Details are provided in (Ref 26).

Stress Analysis near the Weld Pool. At temperatures below 800 to 1200 °C (1470 to 2190 °F) in steel welds, it has often been assumed that the viscous strain, or creep, rate can be neglected in welds, because the time at high temperatures is relatively short. If this assumption is accepted, then the material can be modeled as a thermoelastoplastic material. The theory for this is rather well accepted. Above some temperature, it is expected that the viscous strain, or creep, rate will become important, possibly becoming the dominant deformation mechanism, in which case the material would behave as a viscoelastoplastic material. The theory for this behavior is not well established.

When a solid melts, the material changes from elastic behavior to a viscous fluid. This change is reflected in the Deborah number. It has been argued that even at the melting point, the crystal maintains a yield strength of the order of 5 MPa (0.7 ksi). When it melts, the yield stress drops to zero. Matsunawa (Ref 29) estimated that the viscosity of a liquid increases by a factor of 2×10^{13} upon solidification. The essence of elastic behavior is the existence of a reference state with zero stress. In a crystal, this reference state is crystal lattice. A liquid has no such reference state. Thus, there is a profound change in the physical behavior and the relevant mathematics upon melting. To deal with the change, the liquid and solid regions are typically considered as separate problems. On the interface, the temperature and the traction are continuous.

Because the authors do not know of any careful stress analysis in this temperature range for welds, this problem is left open.

Stress Analysis of Welds in Thin-Walled Structures. The use of plate and shell FEM elements can reduce cost and improve numerical accuracy significantly (Ref 30, 31). These elements usually assume that those stress components that project onto the normal-to-the-midsurface plane are zero, that is, s_{zz}, s_{xz}, and s_{yz} are 0 if the z-axis is normal to the midsurface. In heat-transfer analysis, the projection of the temperature gradient onto the midsurface normal plane is assumed to be 0, that is, $\partial T/\partial z = 0$. This is usually an excellent approximation, except near the intersection of surfaces, such as a pipe T-joint. It can be a good approximation of near-deep-penetration electron-beam and laser-beam welds but is usually not accurate near arc weld pools. Figure 9 shows an example of a weld that would not be accurately approximated by shell elements near the weld pool. Except in such regions, shell and plate elements can be effective. Combining shell and brick elements often provides the best approximation.

Fluid Flow in the Weld Pool

Thus far, weld pool data, that is, an adequate approximation of size, shape, and position, have been known as functions of time. Either the weld pool temperature or the power density and thermal flux distribution also have been known as functions of time. To predict weld penetration, solidification mode and microstructure, and other phenomena that are sensitive to the weld-pool physics, such as hot cracking and the stress and strain near the weld pool, it is necessary to model the weld pool. The model should predict the temperature, pressure, and velocity distribution in the weld pool, as well as the position of the liquid-solid and

liquid-plasma boundaries. It is also desirable to predict the current density, velocity, and pressure fields in the arc. Matsunawa (Ref 29) presents an excellent review of weld-pool analyses.

The major forces that drive convection in the weld pool are electromagnetic, gravitational or buoyancy, surface tension, and aerodynamic drag. The electromagnetic and gravitational forces act on the interior of the weld pool, whereas the surface tension and aerodynamic drag forces act on the surface, producing a traction force.

The conservation of mass, or continuity, equation for an incompressible liquid in the weld pool is:

$$\nabla \cdot \mathrm{v} = 0 \qquad \text{(Eq 28)}$$

The conservation of momentum in the interior of the weld pool in spatial coordinates is:

$$\rho\dot{\mathrm{v}} + \rho\mathrm{v} \cdot \nabla\mathrm{v} + \nabla p + \nabla \cdot \mu\nabla\mathrm{v} + \mathbf{J} \times \mathbf{B} + f \qquad \text{(Eq 29)}$$

where ρ is the density, and p is the pressure. The boundary conditions on the weld pool and arc interface are the traction that is due to the gradient in the surface tension, $-[(\partial\gamma)/(\partial T)]\nabla_s T$, and the traction, τ_D, that is due to drag from the velocity of the plasma:

$$\sigma \cdot n = -\mu\dot{\epsilon} \cdot n = -\frac{\partial\gamma}{\partial T}\nabla_s T + \tau_D \qquad \text{(Eq 30)}$$

where n is the direction normal to the weld pool and arc interface, and the gradients are gradients in the surface. On the interface between the weld pool and solid, the velocity is zero, and the traction vector is continuous. The pressure must be specified at one point in the weld pool. When dealing with an incompressible fluid, it is important to remember that the pressure is not a thermodynamic variable but a constraint to enforce incompressibility.

The conservation of energy in the interior of the weld pool in spatial coordinates is:

$$\rho\frac{\partial H}{\partial t} + \rho\mathrm{v} \cdot \nabla H = \nabla \cdot \kappa\nabla\mathrm{v} + f \qquad \text{(Eq 31)}$$

The velocity in the energy equation is determined from the momentum and continuity equation. The thermal flux from the arc is prescribed on the weld pool and arc interface. With these data, the energy equation determines the position of the liquid-solid interface. With a new temperature distribution, the momentum equation is solved. If this iteration procedure converges, then the result is said to be a solution.

The mathematical nature of the aforementioned equations that model the weld pool and their numerical solution is significantly more difficult than those needed to model the behavior of welds below, say, 0.7 of the melting temperature. The physics is also more difficult. Most analyses of the weld pool have used either finite-difference or finite-volume methods. They have achieved interesting results and have done much to clarify the physics of the weld pool. However, in Matsunawa's view (Ref 29), the capability to accurately predict weld-pool shape and size is still limited. See Ref 30 and the references therein for more recent research on weld-pool modeling. Continued progress in weld-pool modeling is needed and can be expected.

Acknowledgment

The financial support of the National Science and Engineering Research Council is gratefully acknowledged.

REFERENCES

1. S.A. David, T. DebRoy, J.N. DuPont, T. Koseki, and H.B. Smartt, Ed., Technology and Engineering, *Trends in Welding Research, Proceedings of the Eighth International Conference,* June 2–5, 2008 (Callaway Gardens Resort, Pine Mountain, GA), ASM International, 2009
2. L. Karlsson, Ed., *Mechanical Effects of Welding, IUTAM Symposium* (Luleå, Sweden), International Union of Theoretical and Applied Mechanics, June 1991
3. H. Cerjak, H.K.D.H. Bhadeshia, and N. Enzinger, Ed., *Ninth International Seminar on Numerical Analysis of Weldability,* Sept 28–30, 2009 (Graz-Seggau, Austria)
4. T.H. North, Ed., *Proc. Int. Institute of Welding Congress on Joining Research,* Chapman and Hall, July 1990, p 69–82
5. M. McDill, A. Oddy, and J. Goldak, An Adaptive Mesh-Management Algorithm for Three-Dimensional Automatic Finite Element Analysis, *Can. Soc. Mech. Eng.,* Vol 15 (No. 1), 1991
6. K.J. Bathe, *Finite Element Procedures in Engineering Analysis,* Prentice-Hall, 1982
7. C. Johnson, *Numerical Solution of Partial Differential Equations by the Finite Element Method,* Cambridge Press, 1987
8. T.J.R. Hughes, *The Finite Element Method: Linear and Static and Dynamic Finite Element Analysis,* Prentice-Hall, 1987
9. D. Rosenthal, The Theory of Moving Sources of Heat and Its Application to Metal Treatments, *Trans. ASME,* Vol 68, 1946, p 849–865
10. R.R. Rykalin, Energy Sources for Welding, *Welding in the World,* Vol 12 (No. 9/10), 1974, p 227–248
11. V. Pavelic, R. Tanbakuchi, O.A. Uyehara, and P.S. Myers, Experimental and Computed Temperature Histories in Gas Tungsten-Arc Welding Thin Plates, *Weld. J. Res. Suppl.,* Vol 48, 1969, p 295s–305s
12. J.A. Goldak, A. Chakravarti, and M.J. Bibby, A New Finite Element Model for Welding Heat Sources, *Trans. AIME,* Vol 15B, June 1984, p 299–305
13. J. Goldak, M.J. Bibby, and M. Gu, Heat and Fluid Flow in Welds, *Proc. Int. Institute of Welding Congress on Joining Research,* T.H. North, Ed., Chapman and Hall, July 1990, p 69–82
14. M. Gu and J. Goldak, Steady State Thermal Analysis of Welds with Filler Metal Addition, *Can. Metall. Q.,* Vol 32, 1993, p 49–55
15. J.B. Leblond, Three-Dimensional Simulation of a Laser Surface Treatment through Steady State Computation in the Heat Source's CoMoving Frame, *Proc. Modeling of Casting, Welding and Advanced Solidification* (Davos, Switzerland), TMS, Sept 1990
16. R.I. Karlsson and B.L. Josefson, Three Dimensional Finite Element Analysis of Temperature and Stresses in Single-Pass Butt Welded Pipe, *J. Pressure Vessel Technol. (Trans. ASME),* Vol 11 (No. 2), Feb 1990, p 76–84
17. J.S. Kirkaldy and D. Venoguplan, *Phase Transformations in Ferrous Alloys,* A.R. Marder and J.L. Goldenstein, Ed., AIME, 1984, p 125–148
18. C. Henwood, M.J. Bibby, J.A. Goldak, and D.F. Watt, Coupled Transient Heat Transfer-Microstructure Weld Computations, *Acta Metall.,* Vol 36 (No. 11), 1988, p 3037–3046
19. M. Gu and J. Goldak, Modelling the Evolution of Microstructure in the Heat-Affected Zone, *Can. Metall Q.,* Vol 32 (No. 4), 1993, p 351–362
20. R.A. Vandermeer, Modeling Diffusional Growth during Austenite Decomposition to Ferrite in Polycrystalline Fe-C Alloys, *Acta Metall.,* Vol 38 (No. 12), 1990, p 2461–2470
21. D.G. Tecco, The Effects of Micro-Alloy Level over the Kinetics of Grain Growth in Low-C HSLA Heat-Affected Zones, *Proc. Int. Trends in Welding Research* (Gatlinburg, TN), S. David and J. Vitek, Ed., ASM International, June 1992
22. J.C. Simo, Numerical Analysis of Classical Plasticity, *Handbook for Numerical Analysis,* Vol IV, P.G. Ciarlet and J.J. Lions, Ed., Elsevier, Amsterdam, 1998
23. L.E. Malvern, *Introduction to the Mechanics of a Continuous Medium,* Prentice-Hall, 1969
24. M.E. Gurtin, *An Introduction to Continuum Mechanics,* Academic Press, 1981
25. J.B. Leblond, G. Mottet, and J.C. Devauz, A Theoretical and Numerical Approach to the Plastic Behavior of Steels during Phase Transformations—I. Derivation of General Relations, *J. Mech. Phys. Solids,* Vol 34 (No. 4), 1986, p 395–409
26. A.S. Oddy, J.A. Goldak, and J.M. McDill, Numerical Analysis of Transformation Plasticity in 3D Finite Element Analysis of Welds, *Euro. J. Mech.,* Vol 9 (No. 3), 1990, p 253–263

27. D.A. Corrigan, "Thermomechanical Effects in Fusion Welding of High Strength Steels," Ph.D. thesis, Massachusetts Institute of Technology, 1966
28. H.D. Hibbit and P.V. Marcal, A Numerical Thermo-Mechanical Model for the Welding and Subsequent Loading of a Fabricated Structure, *Comput. Struct.,* Vol 3, 1973, p 1145–1174
29. A. Matsunawa, Modeling of Heat and Fluid Flow in Arc Welding, *Proc. Int. Trends in Welding Research* (Gatlinburg, TN), S. David and J. Vitek, Ed., ASM International, June 1992
30. L. Lindgren and L. Karlsson, Deformations and Stresses in Welding of Shell Structures, *Int. J. Num. Meth. Eng.,* Vol 25, 1988, p 635–655
31. M. Gu, J. Goldak, and K. Haaland, Mixing Thermal Shell and Brick Elements in FEA of Welds, *Proc. Offshore Mechanics and Arctic Engineering Conference* (Stavanger, Norway), ASME, June 1991